Electronic Supplementary information

Dual role of arsenite in hydrolysis and post-hydrolysis fluorescence sensing of selective pH-dependent probe

Pushpendra Singh and Kalyan K. Sadhu*

Department of Chemistry, Indian Institute of Technology Roorkee, Roorkee – 247667, Uttarakhand, India

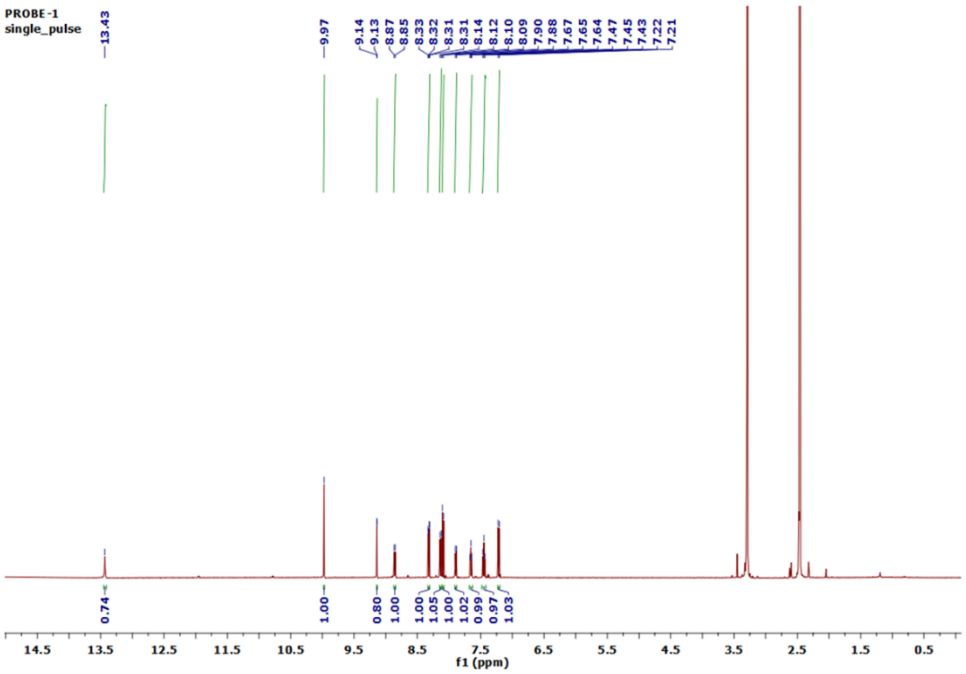

Figure S1. ^{1}H-NMR spectrum of **1** in DMSO-d_6.

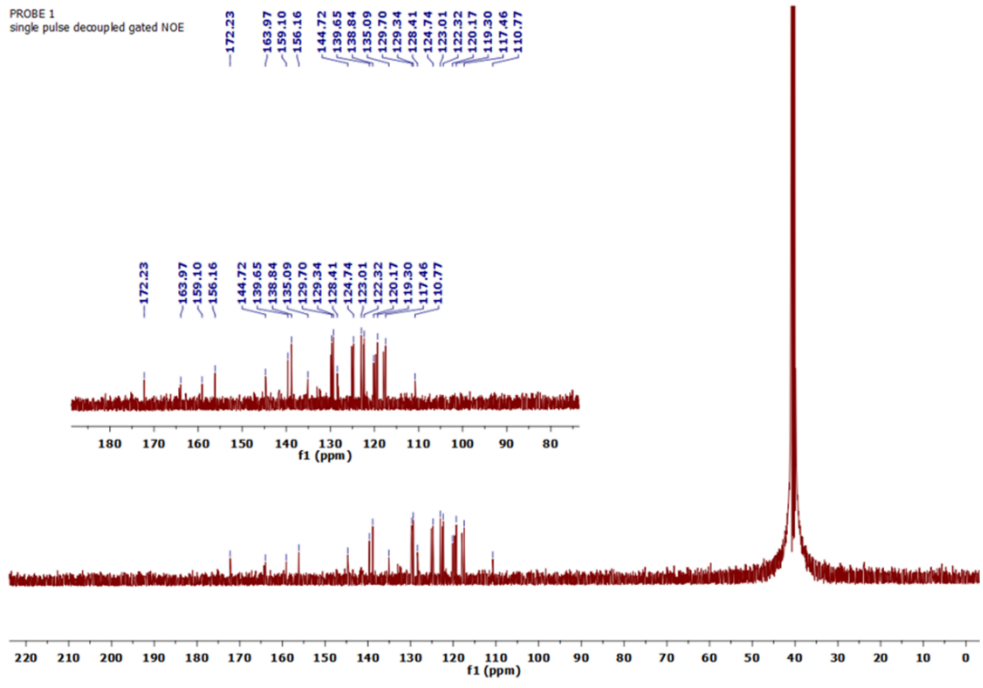

Figure S2. ^{13}C-NMR spectrum of **1** in DMSO-d_6.

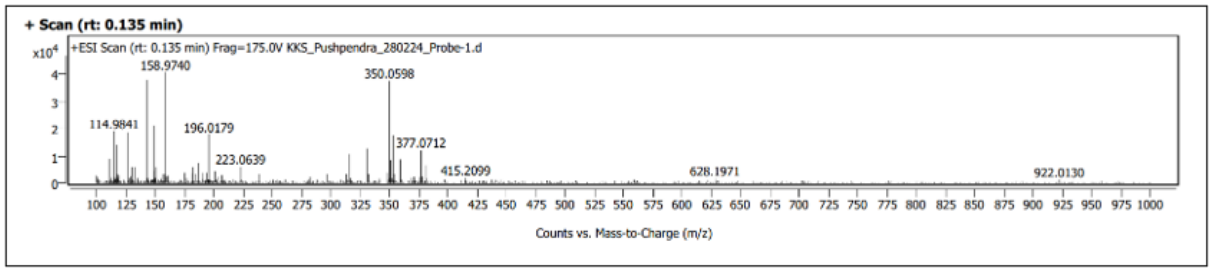

Figure S3. HRMS spectrum of **1.**

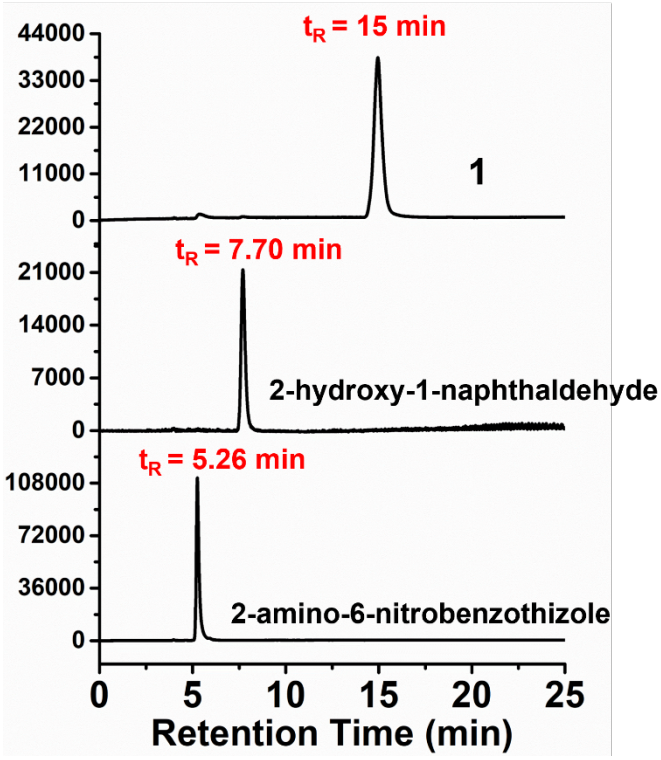

Figure S4. HPLC chromatogram of 2-amino-6-nitrobenzothiazole, 2-hydroxy-1-naphthaldehyde, and **1.**

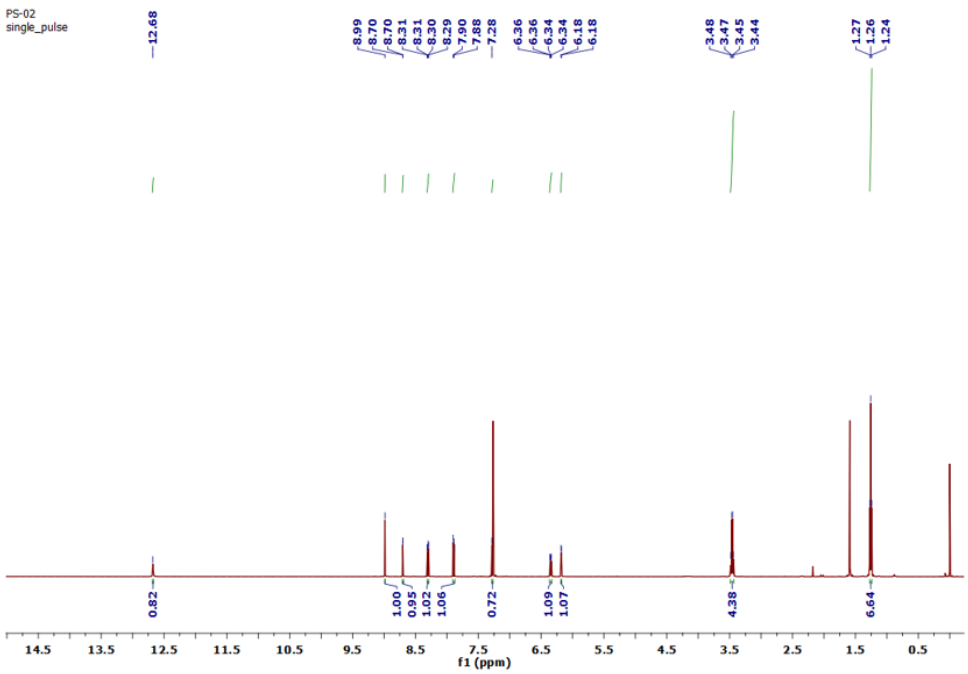

Figure S5. ^{1}H-NMR spectrum of **2** in $CDCl_3$.

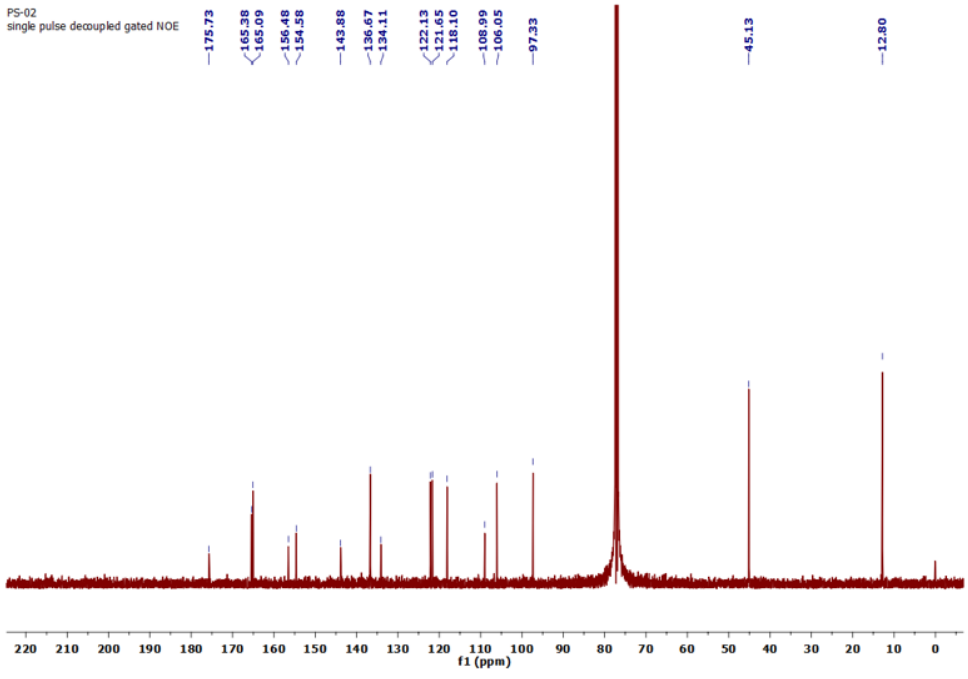

Figure S6. ^{13}C-NMR spectrum of **2** in $CDCl_3$.

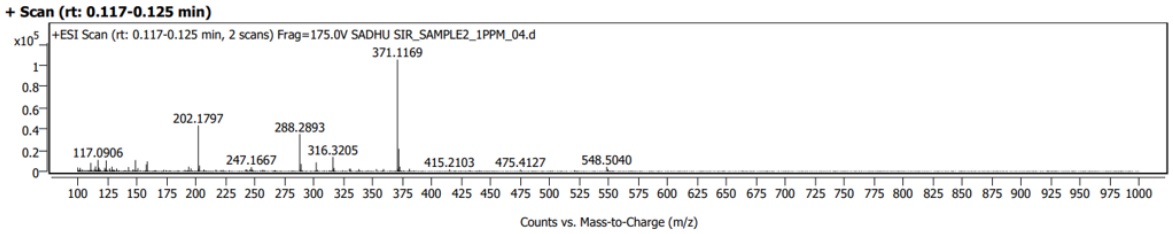

Figure S7. HRMS spectrum of **2**.

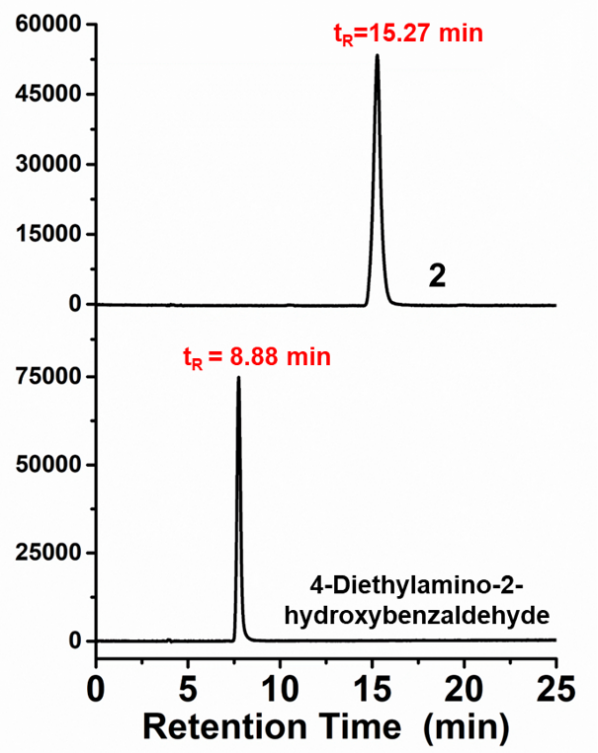

Figure S8. HPLC chromatogram of 4-diethylamino-2-hydroxybenzaldehyde and **2.**

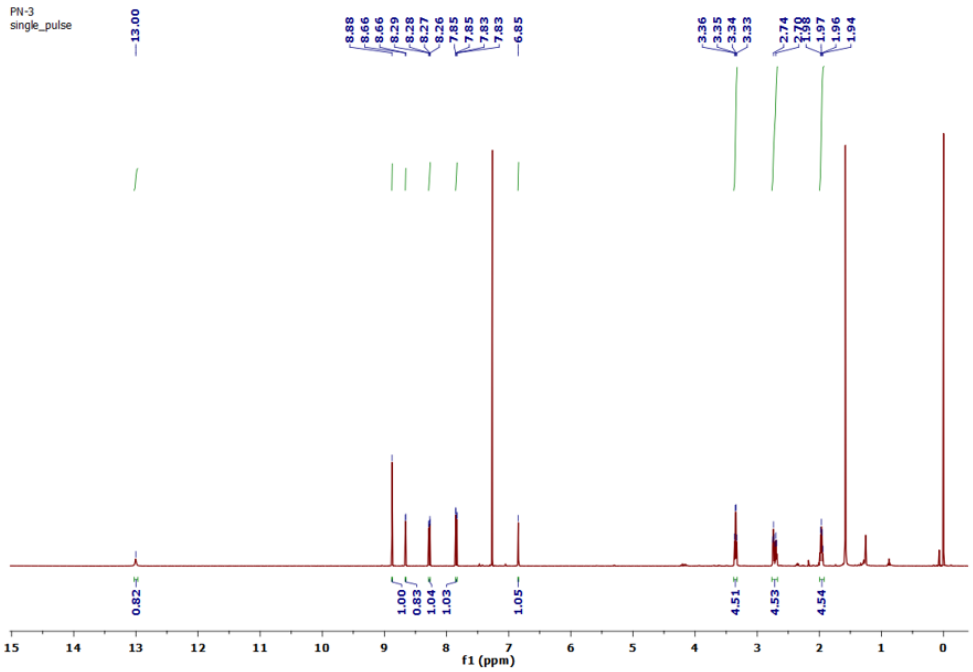

Figure S9. ^{1}H-NMR spectrum of **3** in $CDCl_3$.

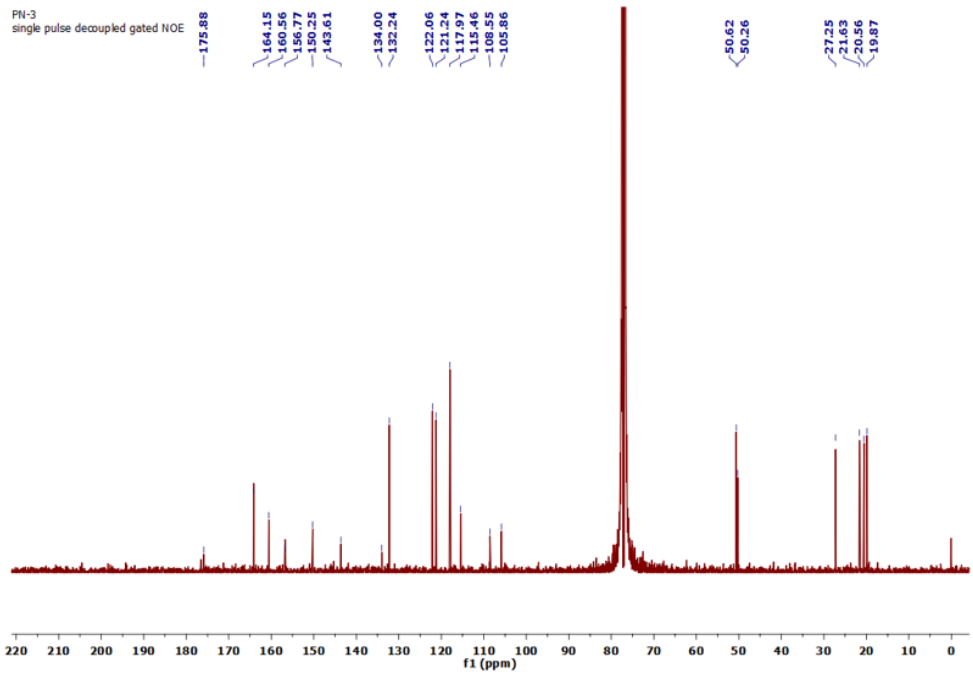

Figure S10. ^{13}C-NMR spectrum of **3** in $CDCl_3$.

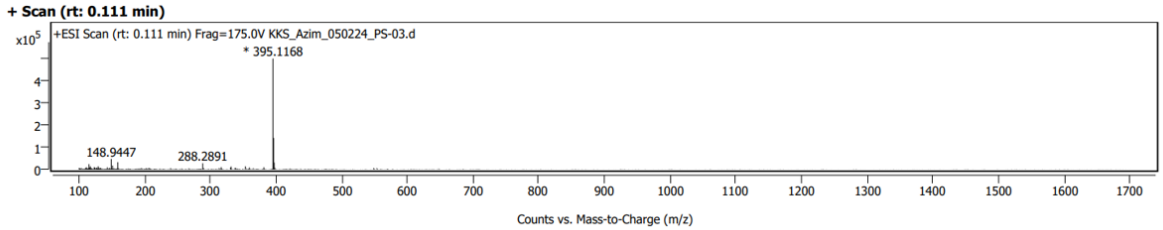

Figure S11. HRMS spectrum of **3**.

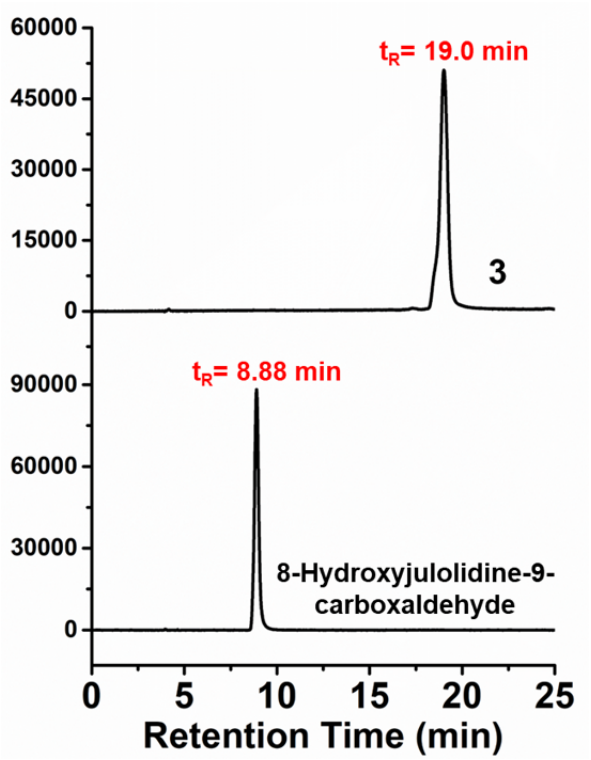

Figure S12. HPLC chromatogram of 8-hydroxyjulolidine-9-carboxaldehyde and **3**.

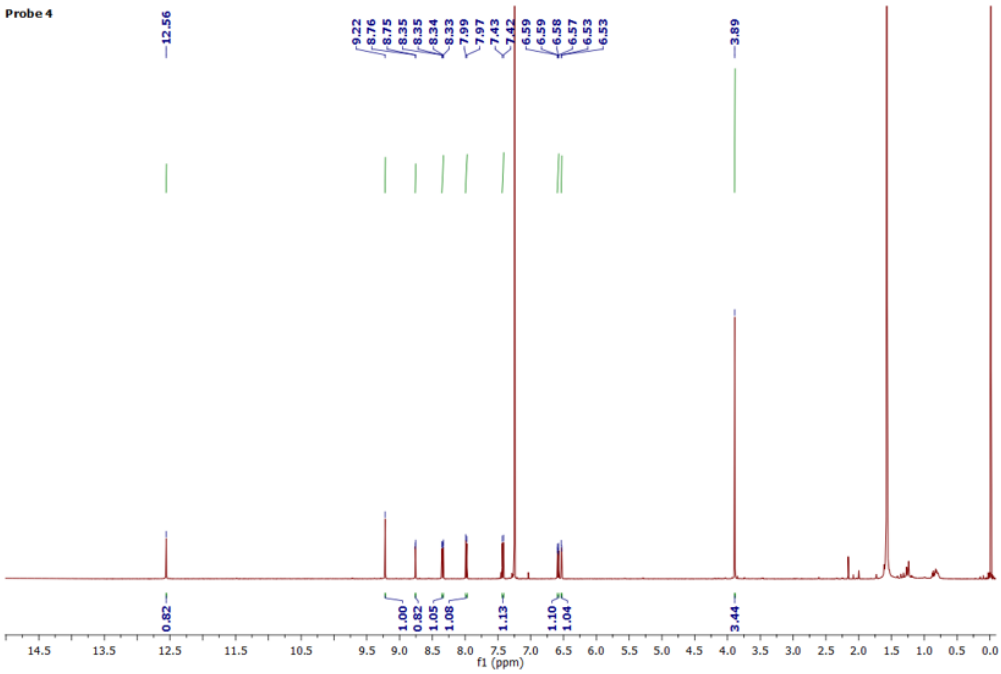

Figure S13. ^{1}H-NMR spectrum of **4** in $CDCl_3$.

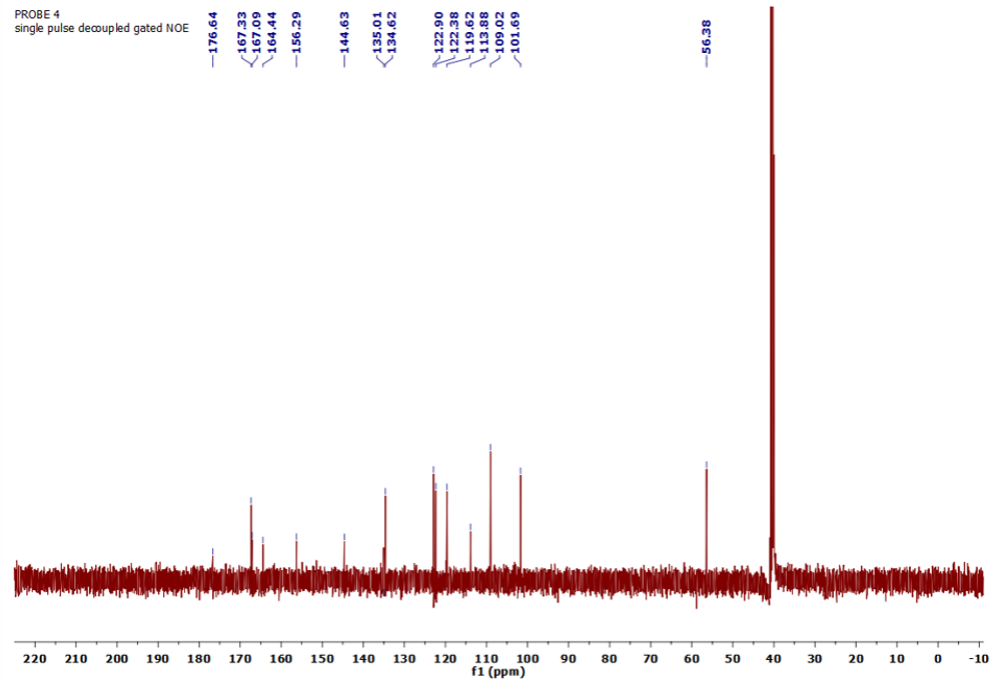

Figure S14. ^{13}C-NMR spectrum of **4** in DMSO-d_6.

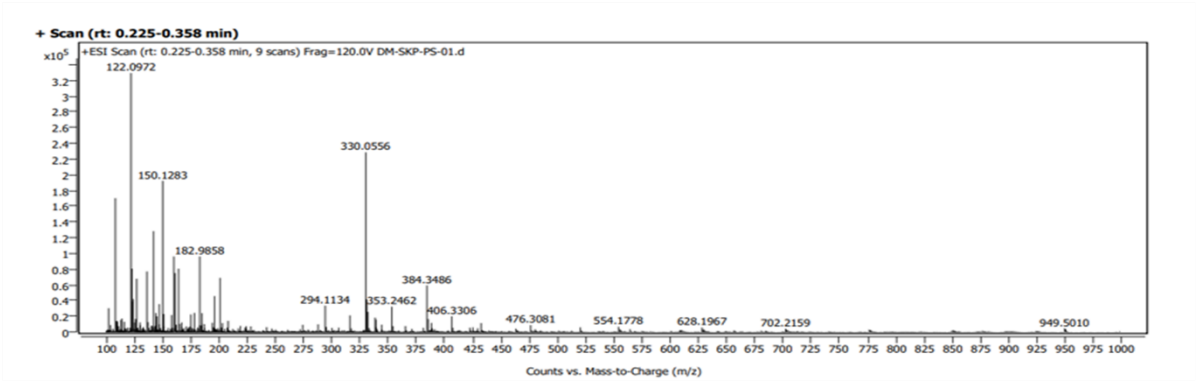

Figure S15. HRMS spectrum of **4**.

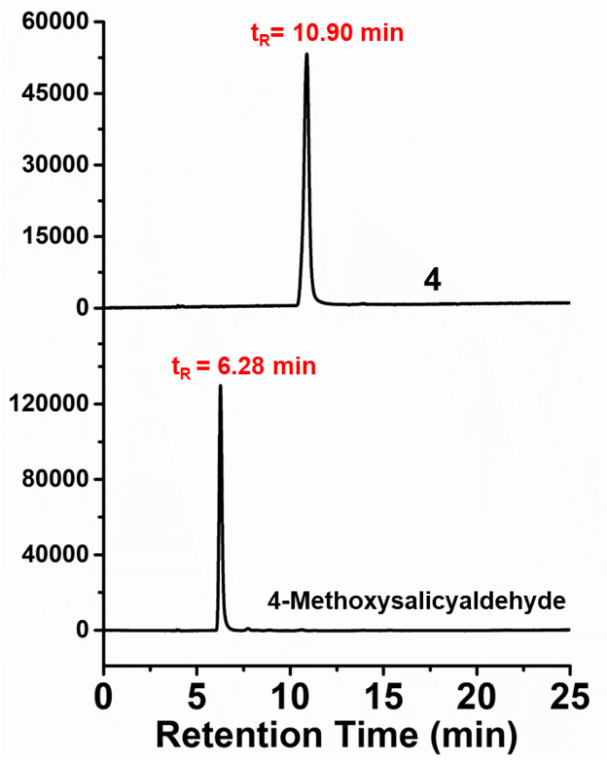

Figure S16. HPLC chromatogram of 4-methoxysalicyaldehyde and **4.**

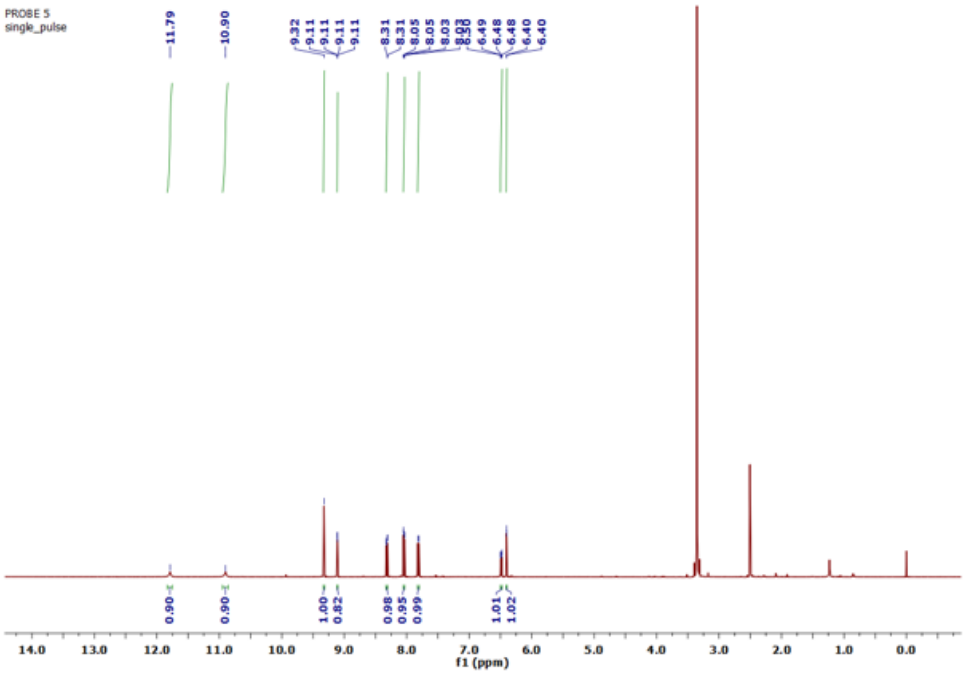

Figure S17. ^{1}H-NMR spectrum of **5** in DMSO-d_6

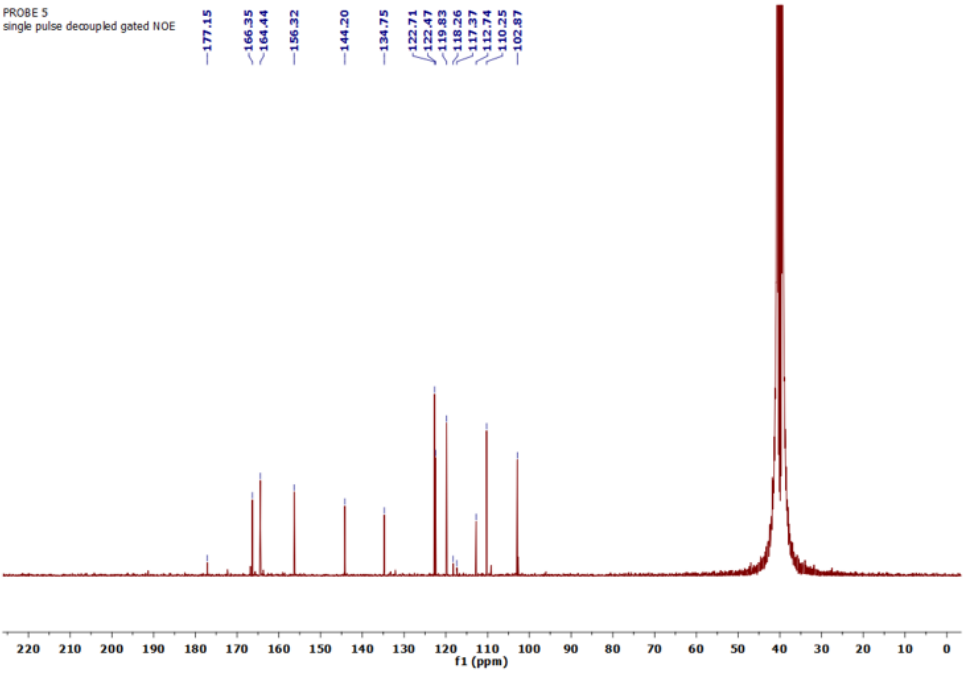

Figure S18. ^{13}C-NMR spectrum of **5** in DMSO-d_6

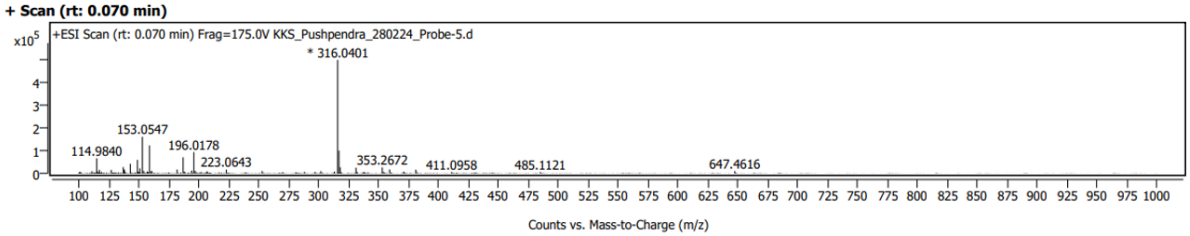

Figure S19. HRMS spectrum of **5**.

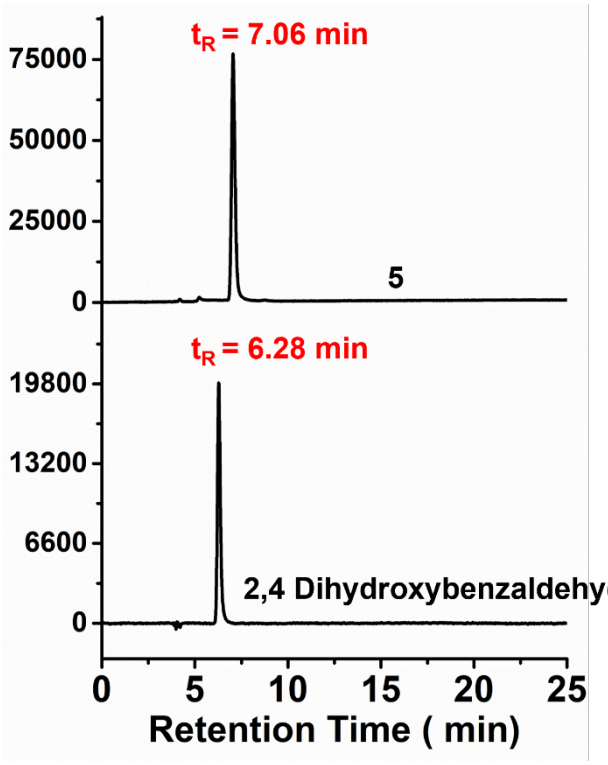

Figure S20. HPLC chromatogram of 2,4-dihydroxybenzaldehyde and **5**.

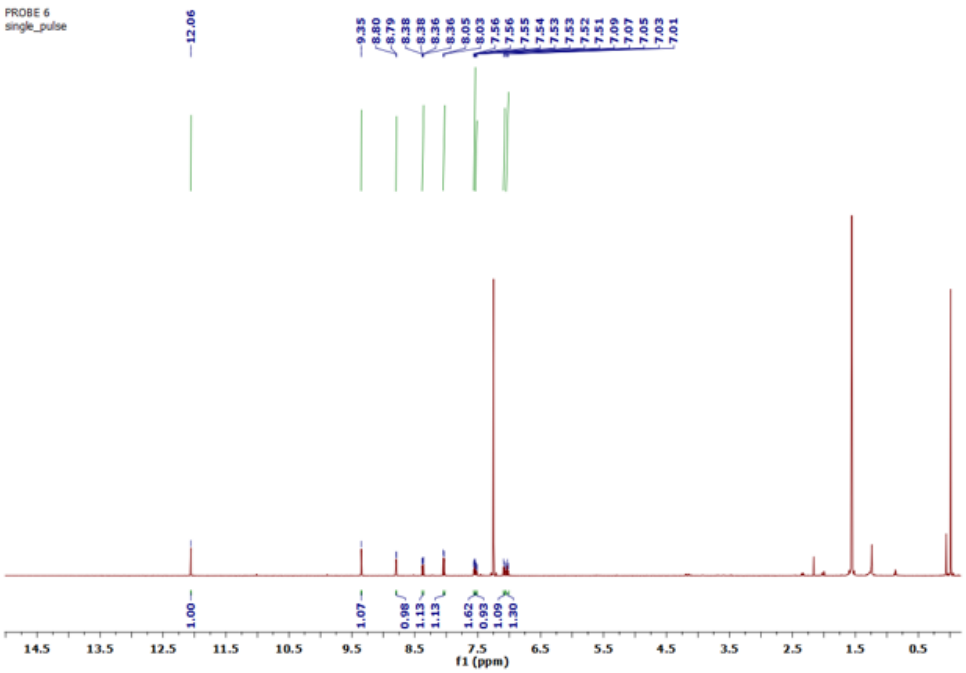

Figure S21. ^{1}H-NMR spectrum of **6** in $CDCl_3$.

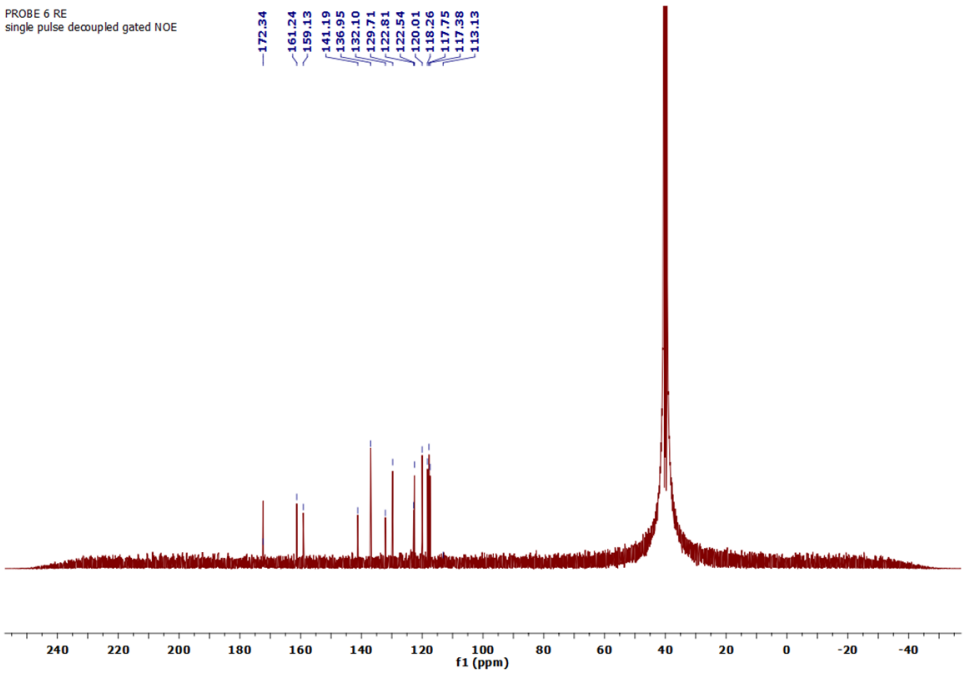

Figure S22. ^{13}C NMR spectrum of **6** in DMSO-d_6.

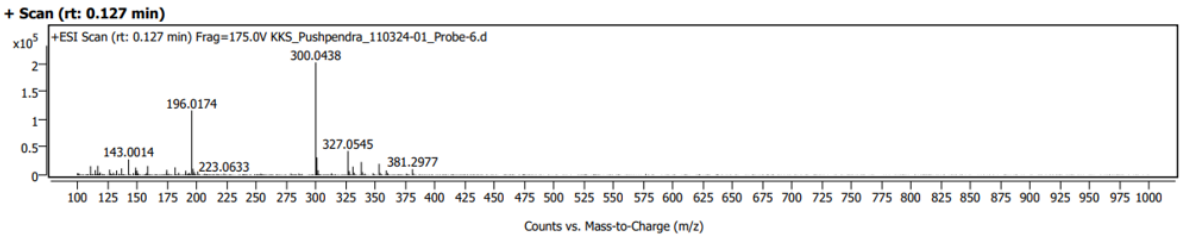

Figure S23. HRMS spectrum of **6.**

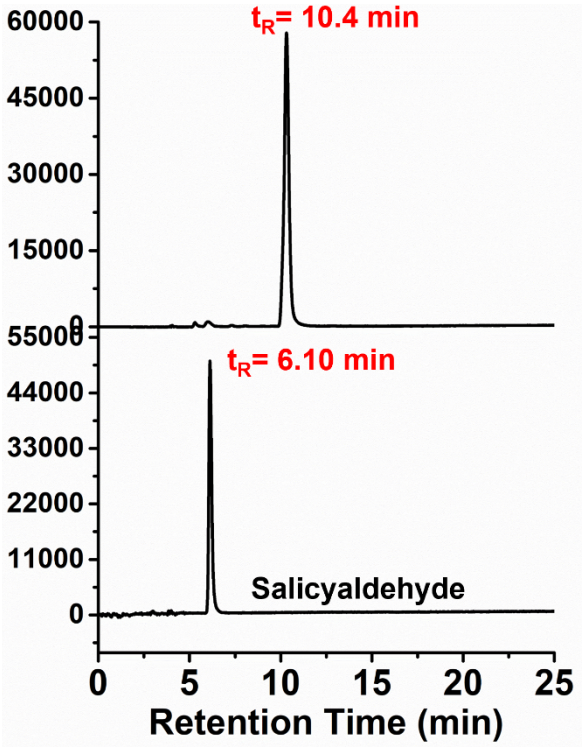

Figure S24. HPLC chromatogram of salicylaldehyde and **6**.

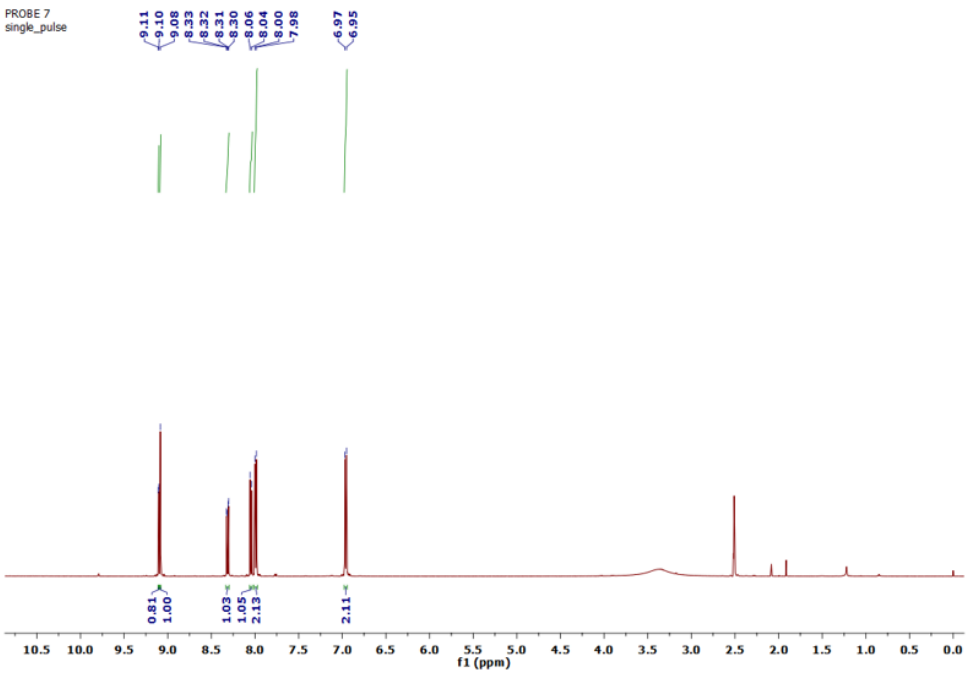

Figure S25. ^{1}H-NMR spectrum of **7** in DMSO-d_6.

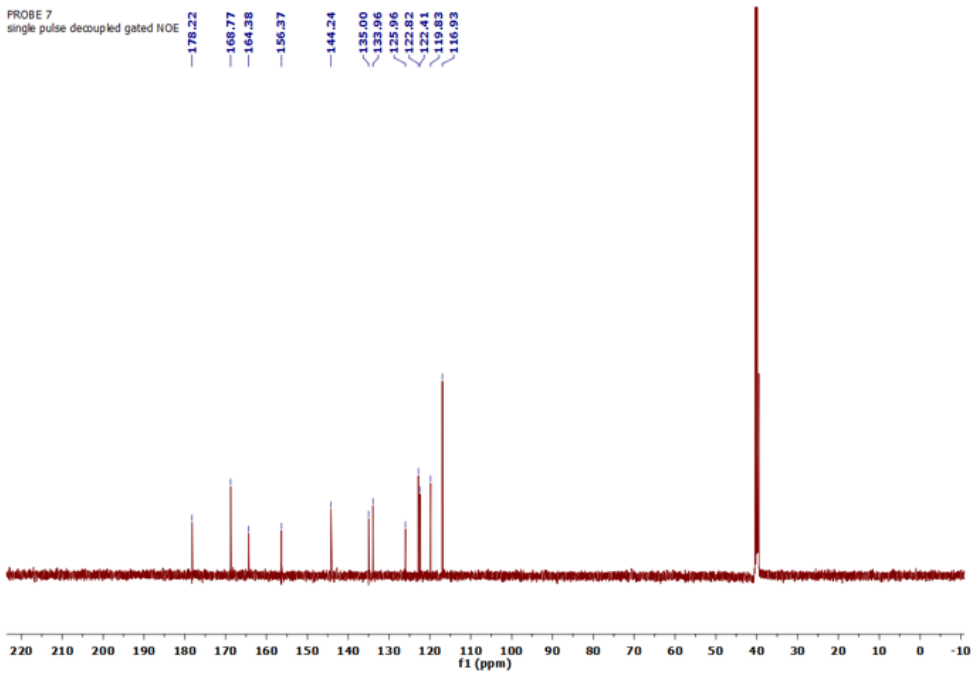

Figure S26. ^{13}C-NMR spectrum of **7** in DMSO-d_6.

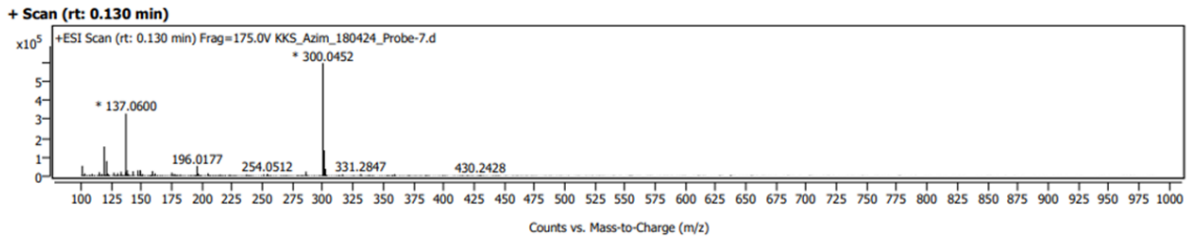

Figure S27. HRMS spectrum of **7**.

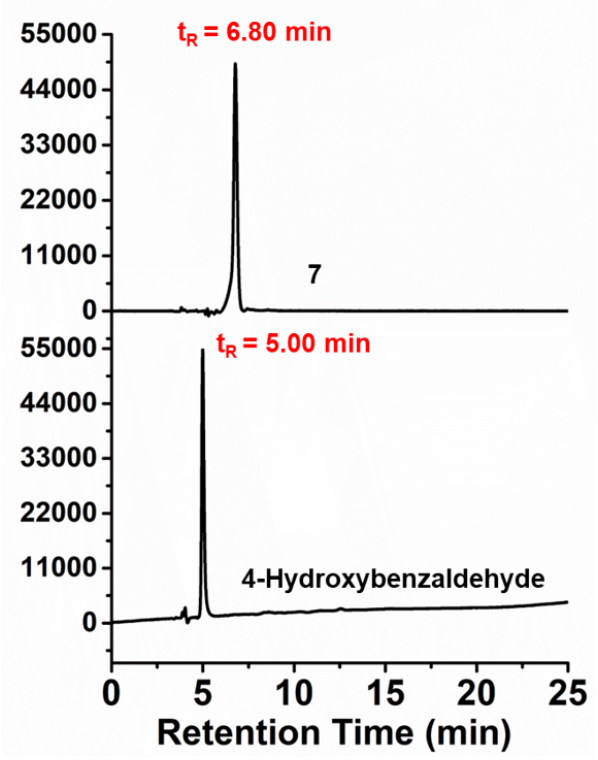

Figure S28. HPLC chromatogram of 4-hydroxybenzaldehyde and **7**.

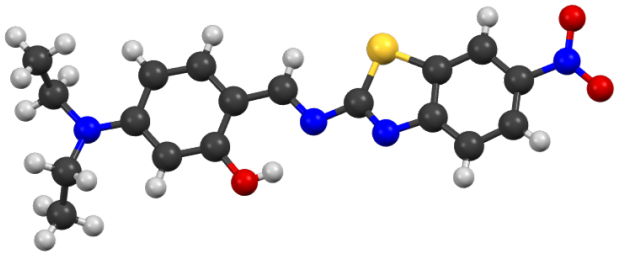

Figure S29. Crystal structure of **2**.

Table S1. Crystallographic information of **2**.

Empirical formula	$C_{17.99}H_{18}N_4O_3S$
Formula weight (g/mol)	370.09 g/mol
Temperature (K)	100(2) K
Crystal System	triclinic
Space group	P -1
Unit cell dimension	a = 6.9321(10) Å, b = 7.3574(10) Å, c = 18.068(3) Å, α = 95.580(9)° β = 97.514(9)° γ = 111.201(9)°
Volume	841.3(2) $Å^3$
Z	2
Density (Calculated) (g/cm^3)	1.461 g/cm^3
Absorbance Coefficient mm^{-1}	0.220 mm^{-1}
F000	388
Crystal Size mm^3	0.010 x 0.030 x 0.256 mm
Theta Range for data collection	2.30 to 25.15°
Index range	$-8 \le h \le 8$, $-8 \le k \le 8$, $-21 \le l \le 21$
Reflections collected	25481
Independent reflections	2978 [R(int) = 0.1602]
Coverage of Independent reflection	99.6%
Absorption correction	Multi-Scan
Max and min transmission	0.9980 and 0.9460
Refinement method	Full-matrix least-squares on F^2
Data/ restrains/ parameters	2978 / 616 / 347
Goodness of fit on F^2	1.070
Final R indices	11769 data; I>2σ(I), R1 = 0.0926, wR2 = 0.1744
R Indices (all data)	R1 = 0.1558, wR2 = 0.2027
Largest diff. peak and hole ($eÅ^{-3}$)	0.540 and -0.376 $eÅ^{-3}$

Table S2. Change in pH of probe **1** (50 μM) with the addition of different anions (500 μM).

	pH		**pH**
Probe 1	6.30	$1 + N_3^-$	8.15
$1 + AsO_2^-$	10.20	$1 + NO_3^-$	6.27
$1 + HAsO_4^{2-}$	9.50	$1 + NO_2^-$	7.60
$1 + PO_4^{3-}$	10.22	$1 + F^-$	9.82
$1 + HPO_4^{2-}$	9.37	$1 + Cl^-$	6.0
$1 + H_2PO_4^{2-}$	5.50	$1 + Br^-$	6.42
$1 + CO_3^{2-}$	10.03	$1 + I^-$	6.12
$1 + HCO_3^-$	10.12	$1 + ClO_4^-$	6.10
$1 + AcO^-$	9.84		
$1 + SO_4^{2-}$	6.58		

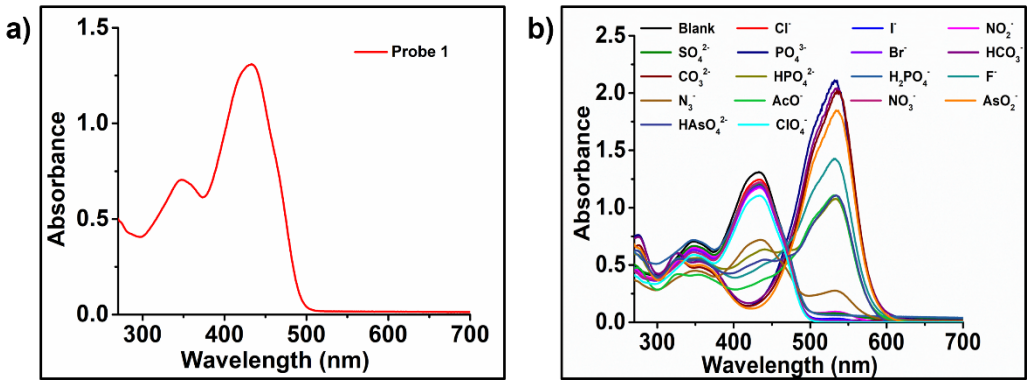

Figure S30. (a) Absorbance spectra of **1** in 5% aqueous acetonitrile; (b) Change absorbance of spectra of **1** with different anions (recorded immediately after the addition of each anion).

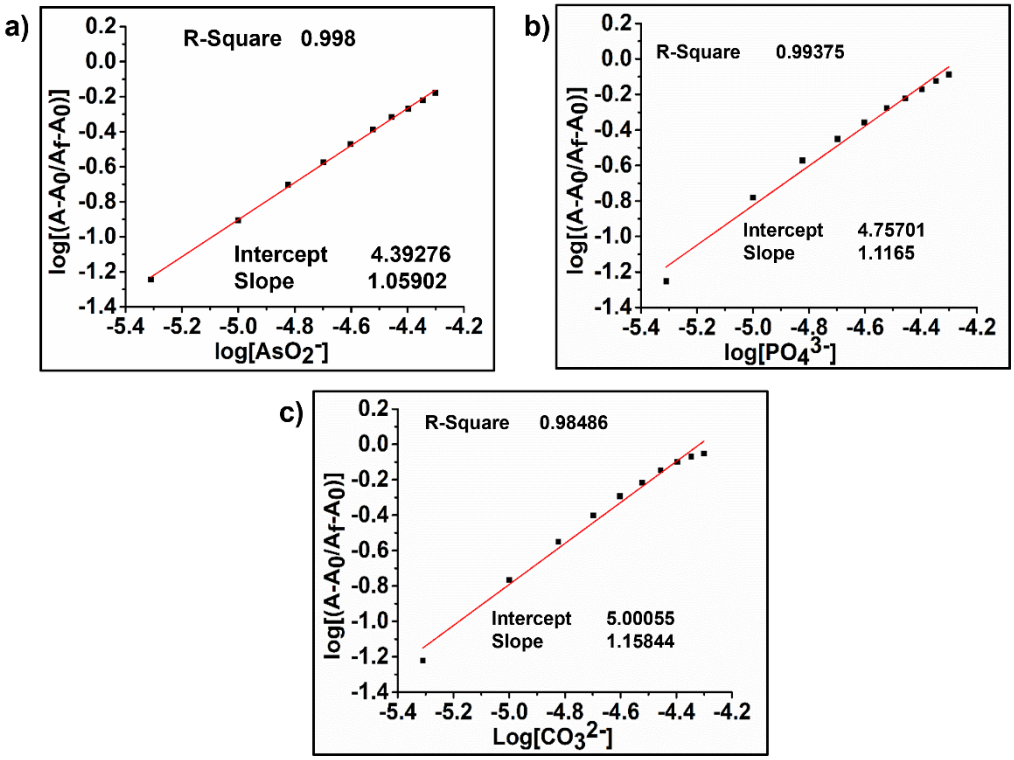

Figure S31. Benesi–Hildebrand plots[1] for calculation of binding constant of **1** for (a) AsO_2^-, (b) PO_4^{3-}, (c) CO_3^{2-}.

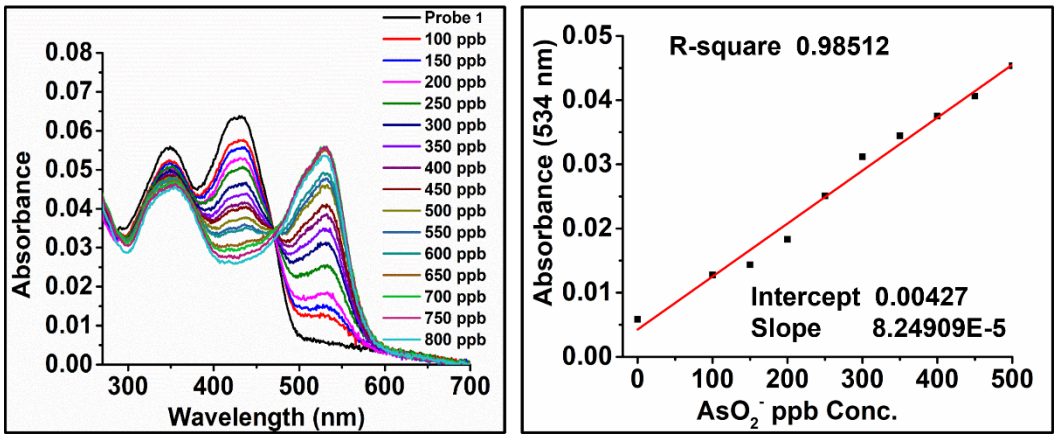

Figure S32. Absorbance response of **1** (1 μM) with (left) ppb conc. of AsO_2^- and (right) calibration curve for calculation of LOD for AsO_2^-.

The limit of detection was calculated by a well-known formula = $3\sigma/S$

where, σ = Standard deviation of blank and S = Slope

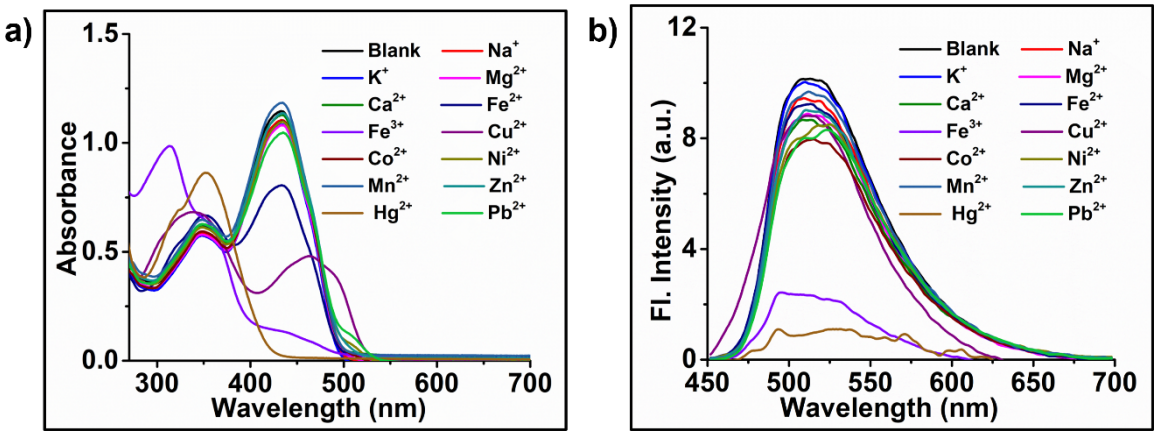

Figure S33. Absorbance (a) and emission (b) of **1** with various cations (λ_{ex} = 420 nm). ClO_4^- is present as counter anion for all the cations.

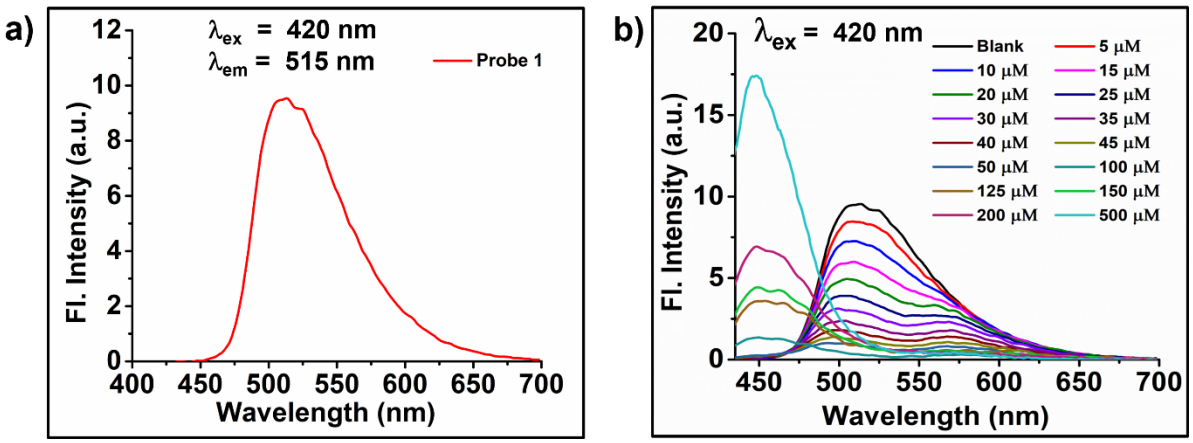

Figure S34. (a) Fluorescence spectrum of **1** (conc. 50 μM) in 5% aqueous acetonitrile; (b) change in the fluorescence spectrum of **1** (conc. 50 μM) with gradually increasing AsO_2^- (0-500 μM).

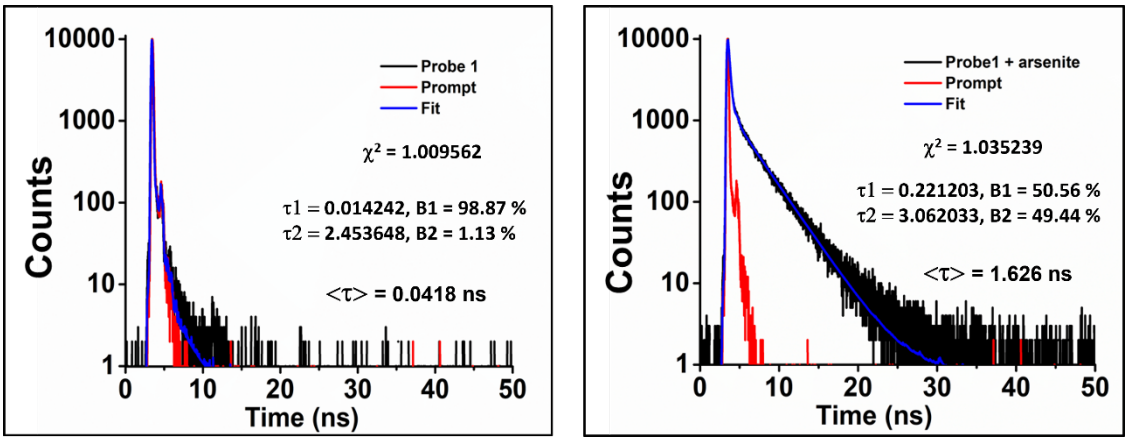

Figure S35. Fluorescence lifetime spectrum of probe **1**, (left) without AsO_2^- ($\lambda_{em.}$= 515 nm) (right) with AsO_2^- ($\lambda_{em.}$= 450 nm) recorded after 10 min. $\lambda_{ex.}$= 405 nm was used in both samples.

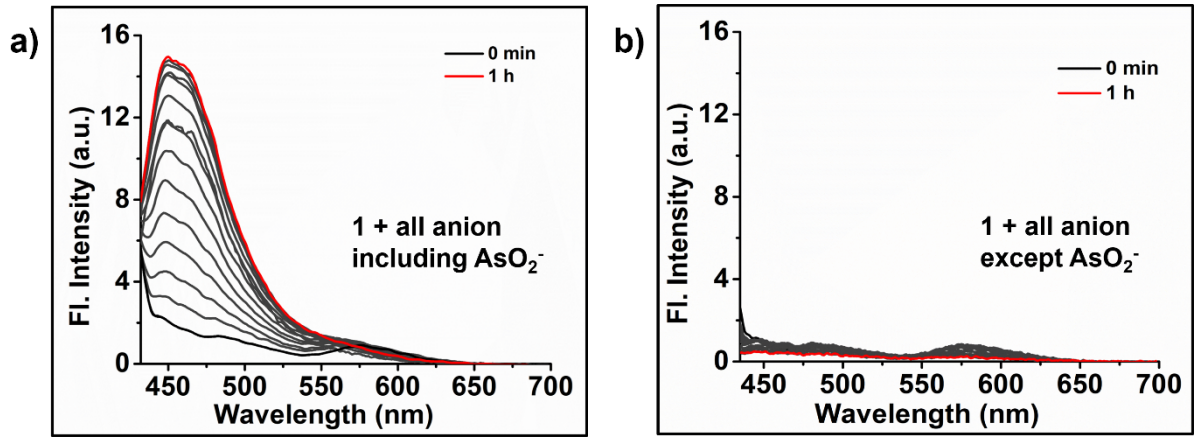

Figure S36. Time-dependent emission spectra of **1** (conc. 50 μM) with all anions (conc. 100 μM) in the (a) presence of AsO_2^- and (b) absence of AsO_2^- (each trace was recorded after 4 min intervals).

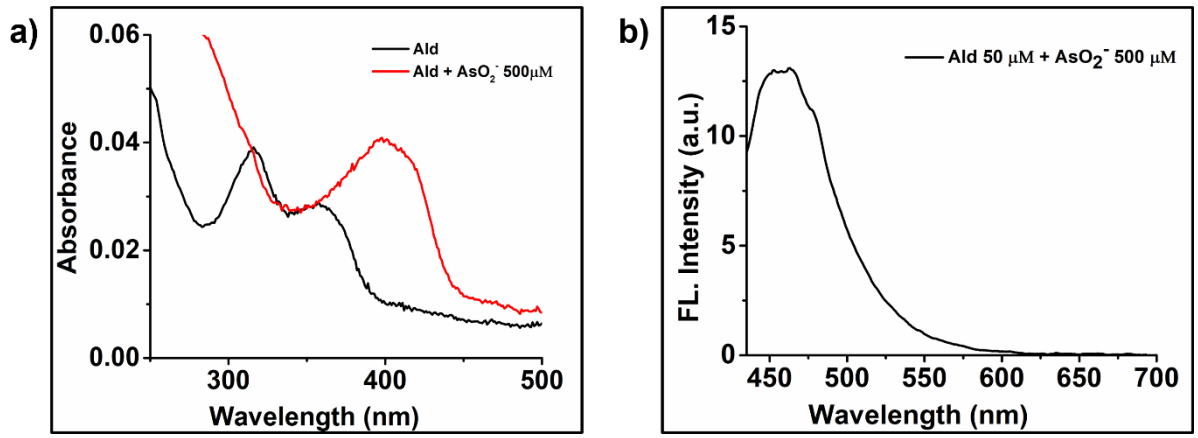

Figure 37. (a) Absorbance and (b) emission spectra (λ_{ex} = 420 nm) of 2-hydroxy-1-naphthaldehyde (50 μM) with addition AsO_2^- (500 μM).

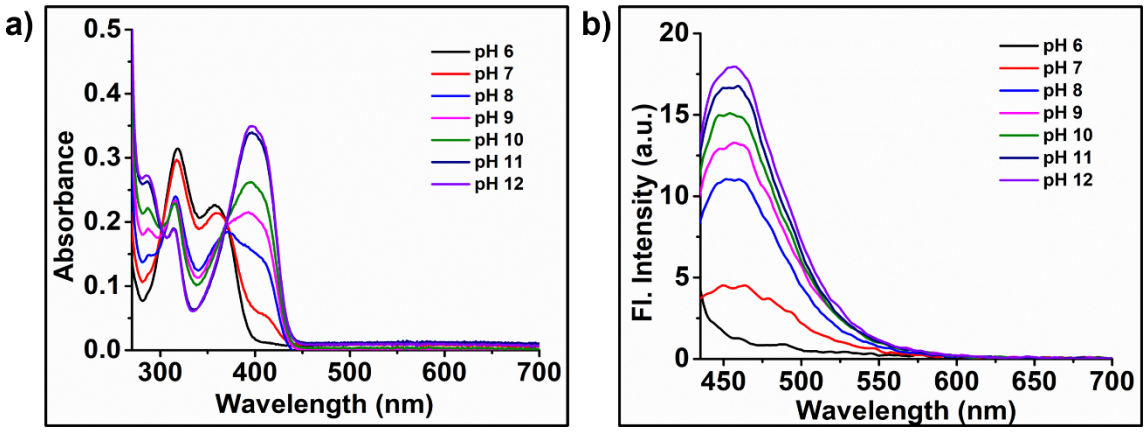

Figure S38. (a) Absorbance and (b) emission spectra (λ_{ex} = 420 nm) of 2-hydroxy-1-naphthaldehyde at different pH.

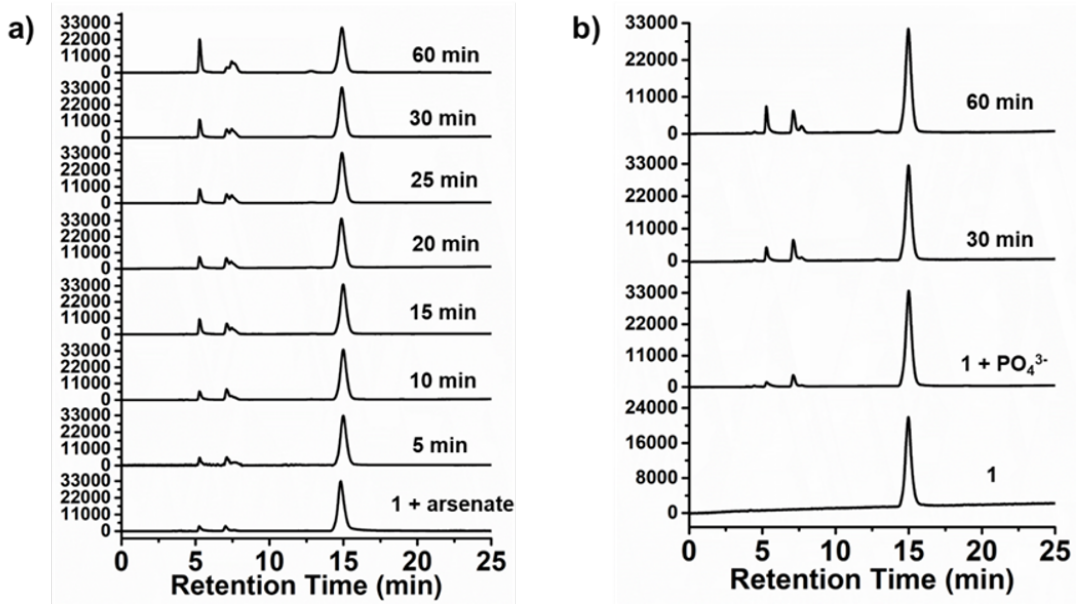

Figure S39. HPLC chromatogram of **1** with (a) AsO_2^- and (b) PO_4^{3-} anions.

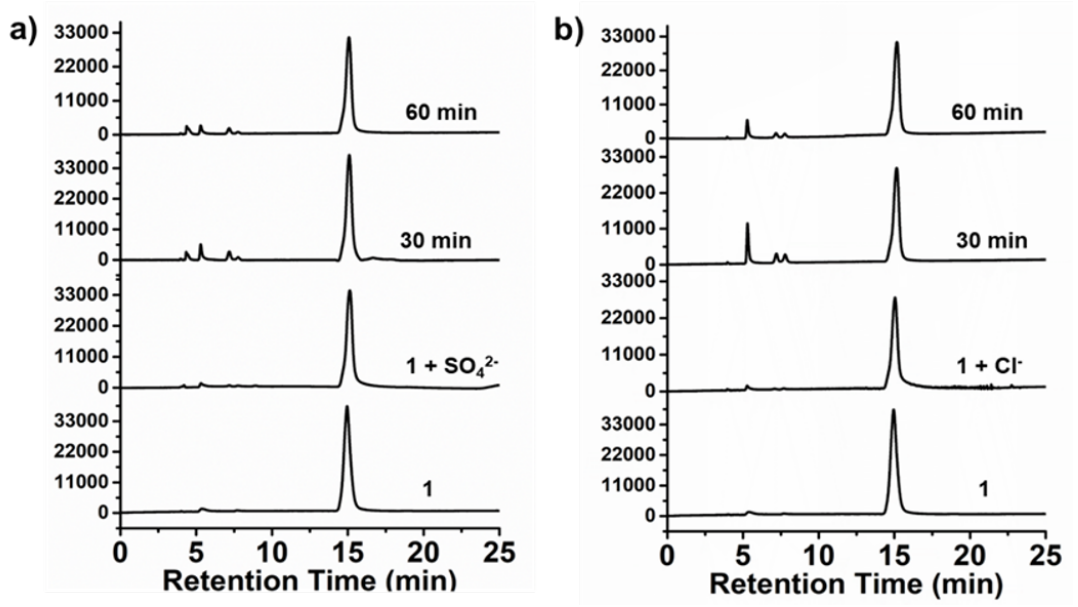

Figure S40. HPLC chromatogram of **1** with (a) SO_4^{2-} and (b) Cl^- anions.

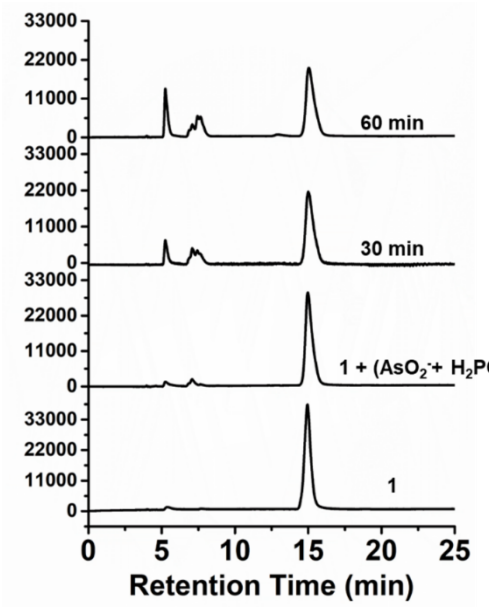

Figure S41. HPLC chromatogram of **1** with (AsO_2^- + $H_2PO_4^-$).

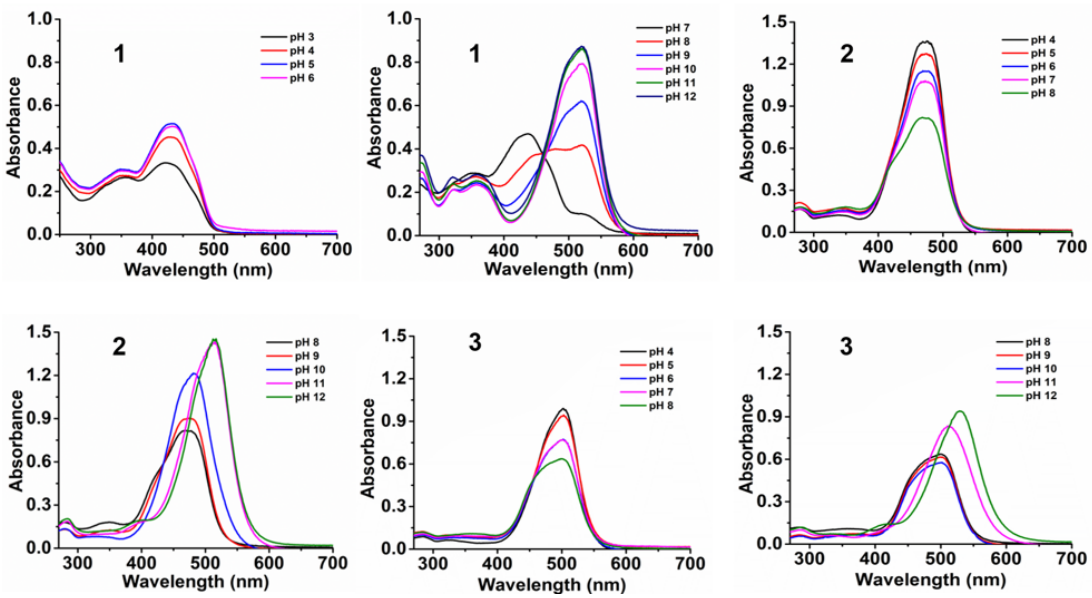

Figure S42. pH response of probes **1**-**3** in buffer.

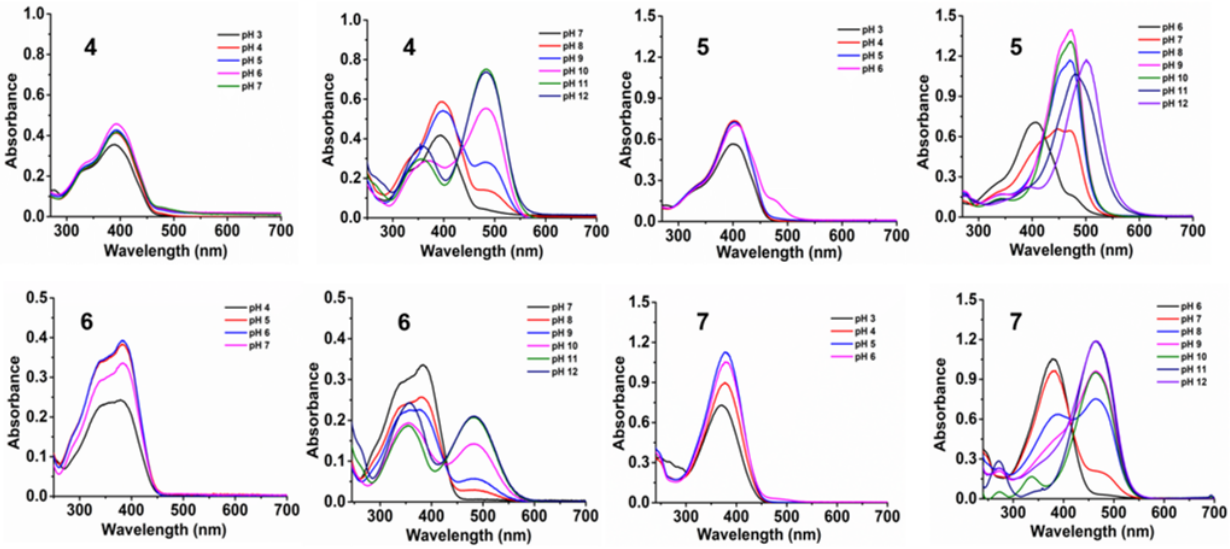

Figure S43. pH response of probe **4**-**7** in buffer.

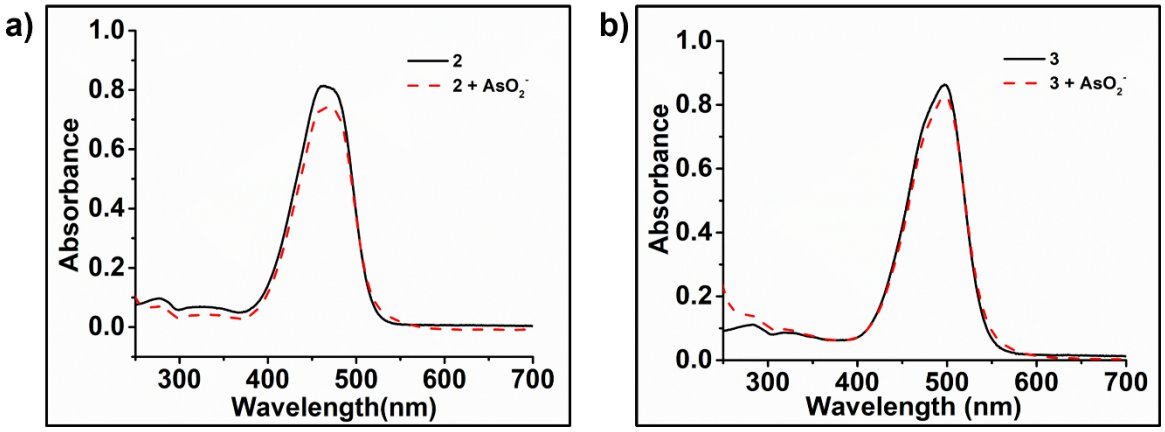

Figure S44. Absorbance spectra of (a) **2** and (b) **3** with and without AsO_2^-.

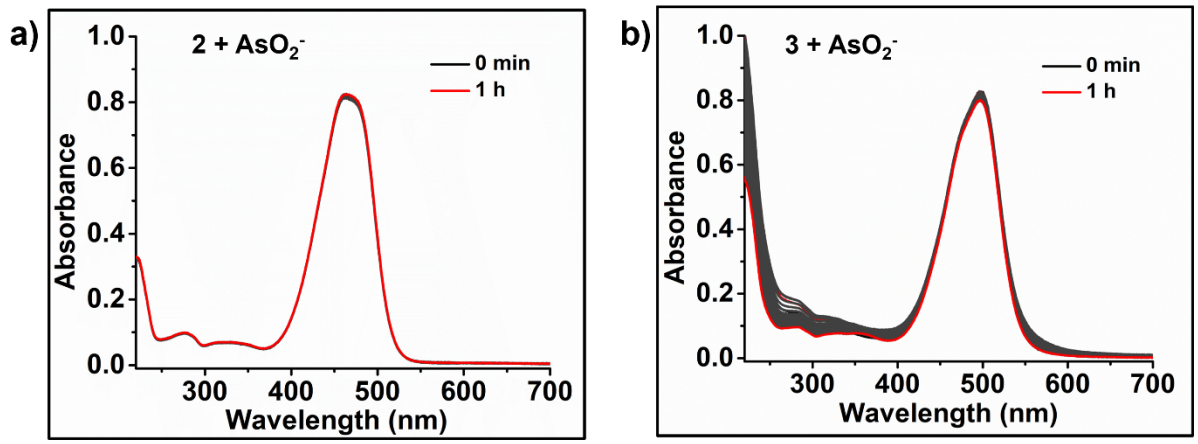

Figure S45. Time-dependent absorbance spectra of (a) **2** and (b) **3** with AsO_2^- (each trace was recorded after 1 min intervals).

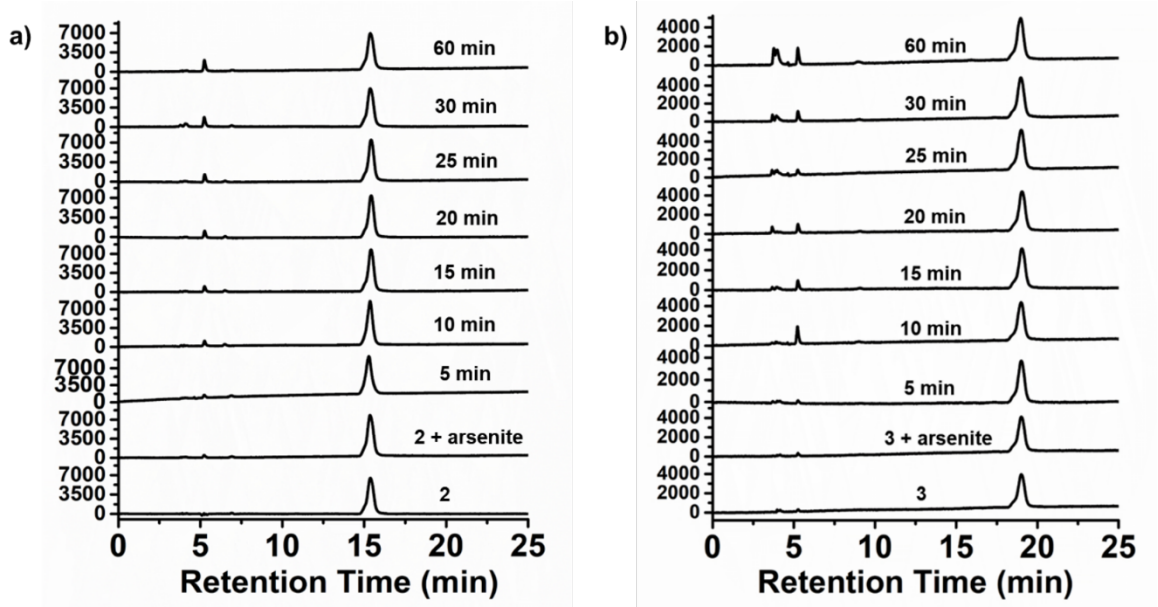

Figure S46. HPLC chromatogram of (a) **2** and (b) **3** with AsO_2^- at different time intervals.

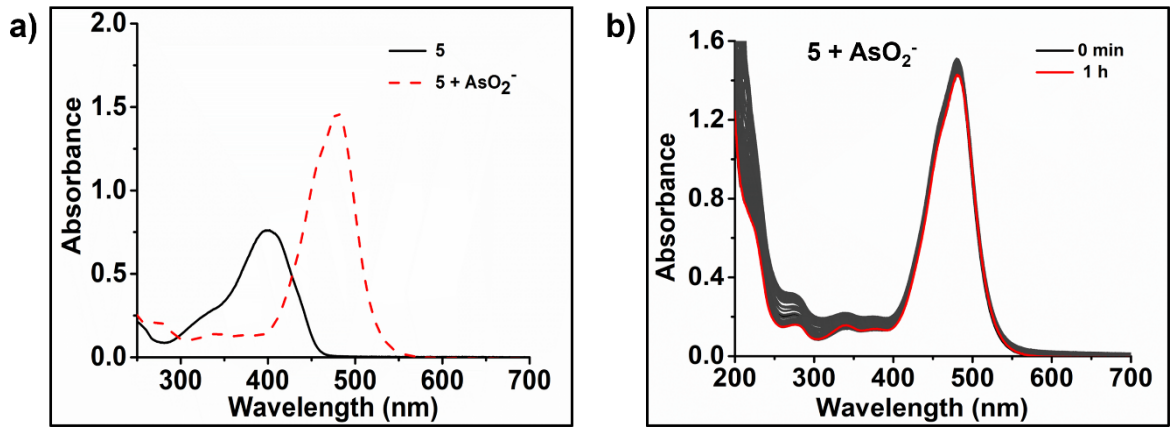

Figure S47. Absorbance spectra of (a) **5** with and without AsO_2^-; (b) time-dependent absorbance spectra of **5** with AsO_2^-(each trace was recorded after 1 min intervals).

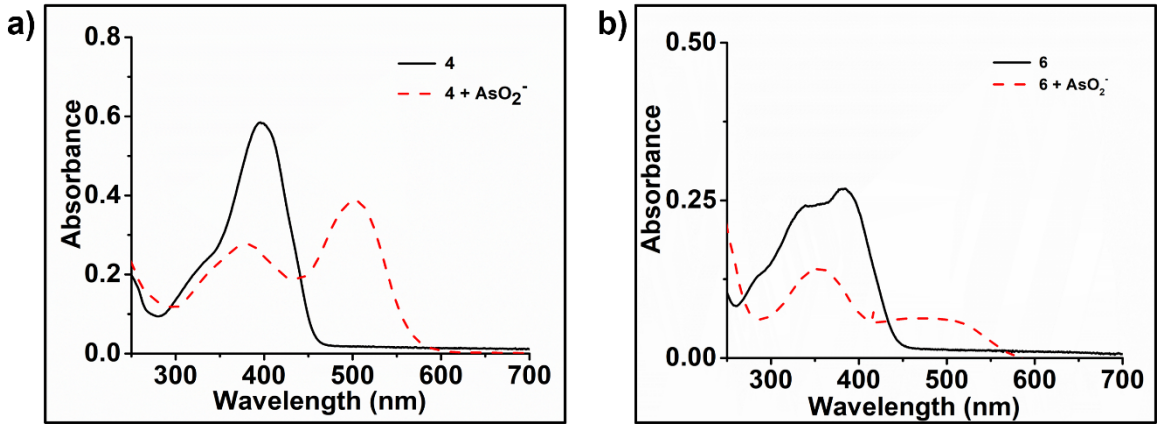

Figure S48. Absorbance spectra of (a) **4** and (b) **6** with and without AsO_2^-.

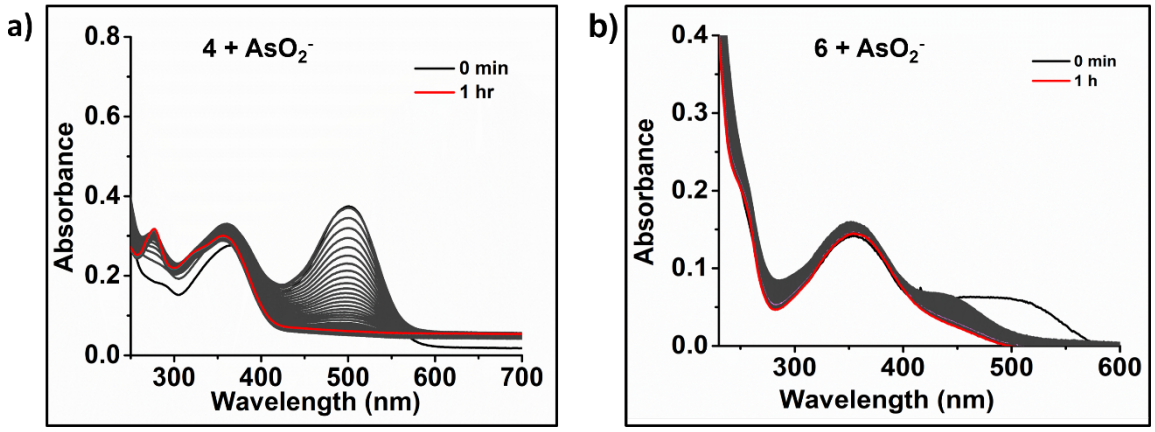

Figure S49. Time-dependent absorbance spectra of (a) **4** and (b) **6** with AsO_2^- each trace was recorded after 1 min intervals.

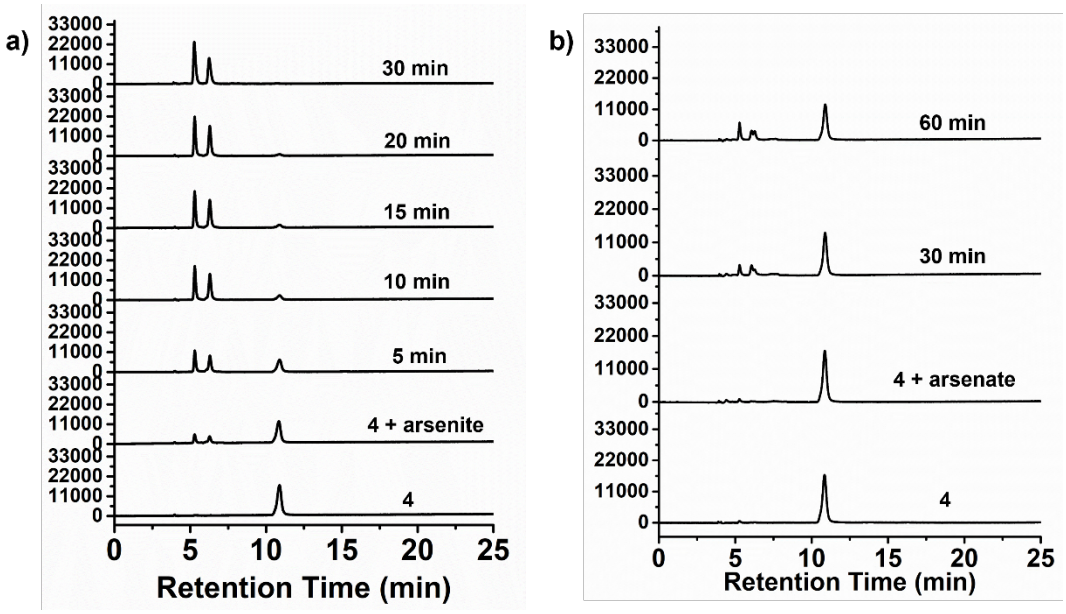

Figure S50. HPLC chromatogram of **4** with (a) AsO_2^- and (b) $HAsO_4^{2-}$ at different time intervals.

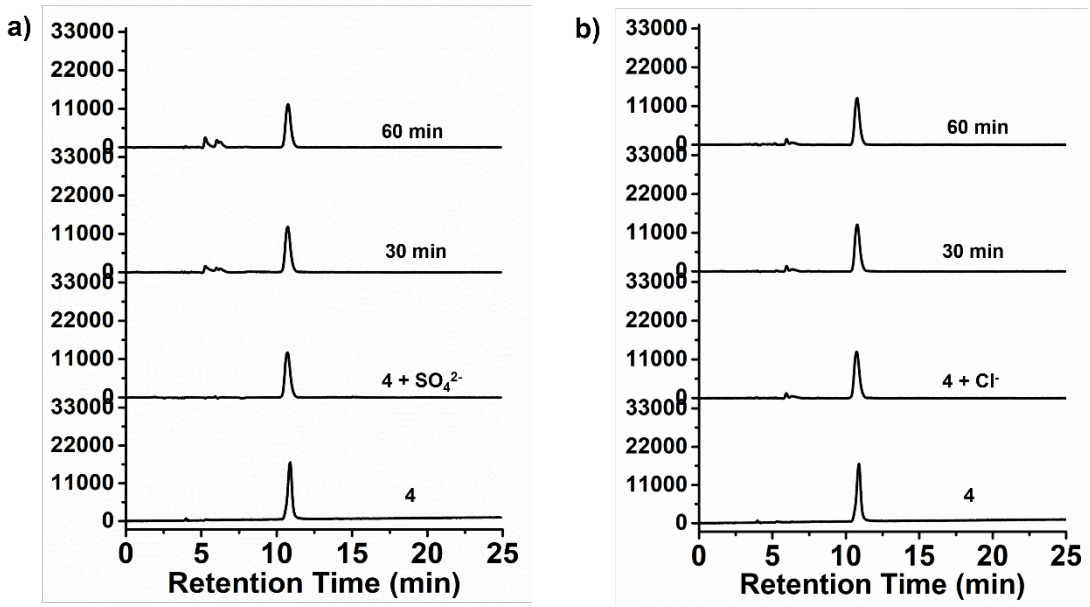

Figure S51. HPLC chromatogram of **4** with (a) SO_4^{2-} and (b) Cl^- at different time intervals.

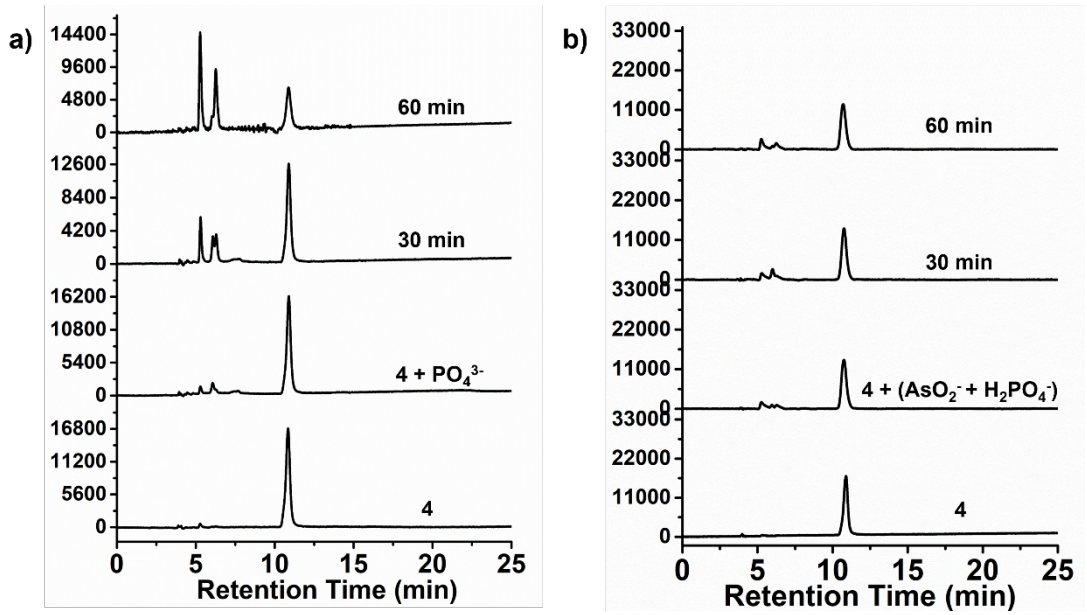

Figure S52. HPLC chromatogram of **4** with (a) PO_4^{3-} and (b) (AsO_2^- + $H_2PO_4^-$) combination.

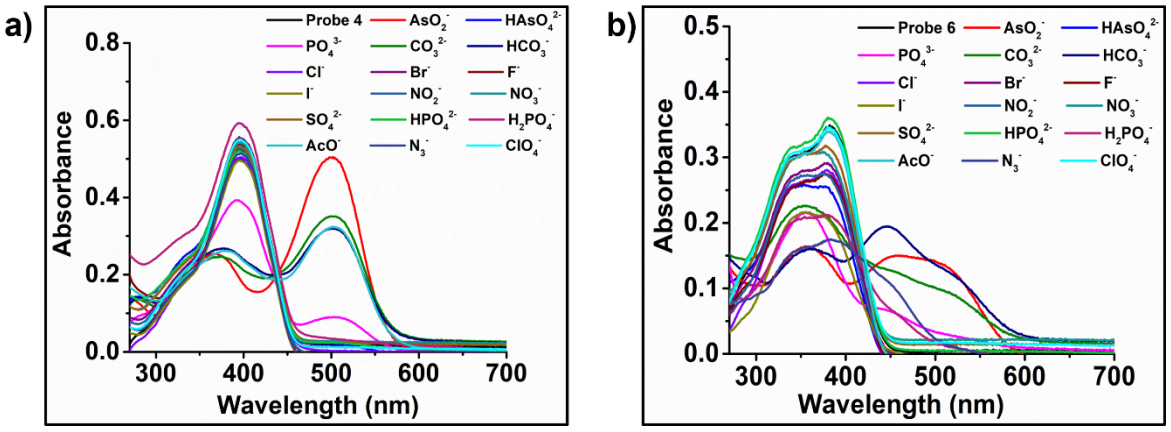

Figure S53. Absorbance spectra of (a) **4** and (b) **6** with different anions were recorded immediately after the addition of each anion.

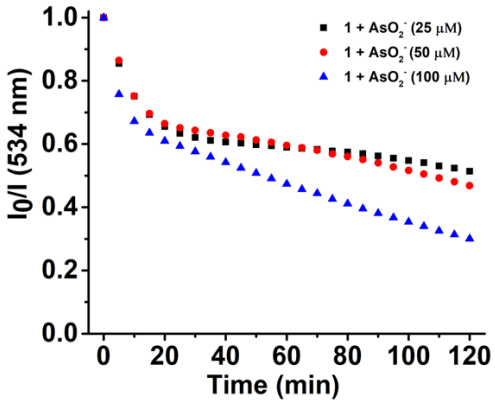

Figure S54. Change in time-dependent absorption spectra of **1** (50 μM) with variable concentration of AsO_2^-.

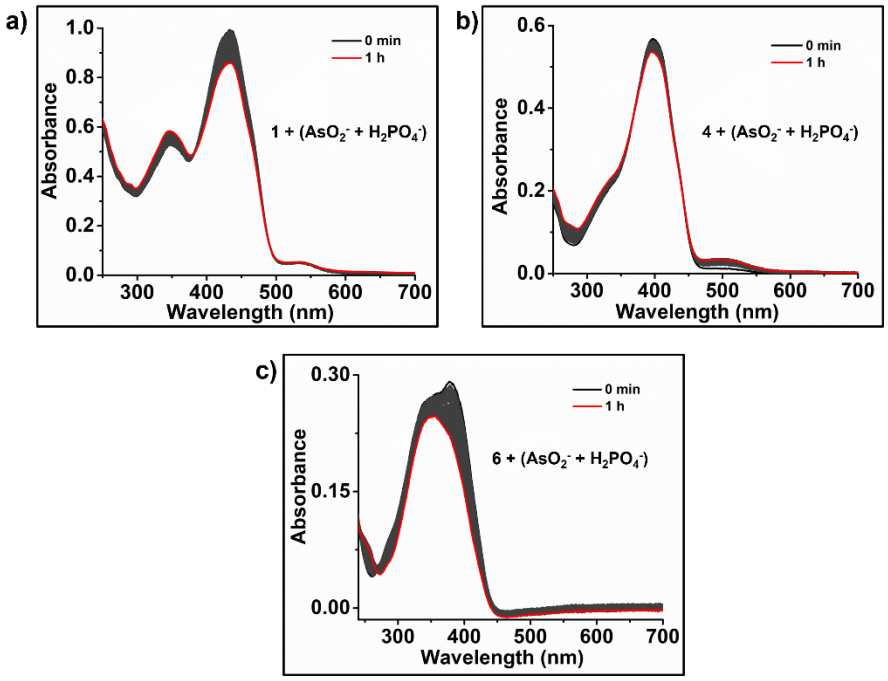

Figure S55. Time-dependent absorption spectra of (a) **1**, (b) **4,** and (c) **6** with (AsO_2^- + $H_2PO_4^-$) combination (each trace was recorded after 1 min intervals).

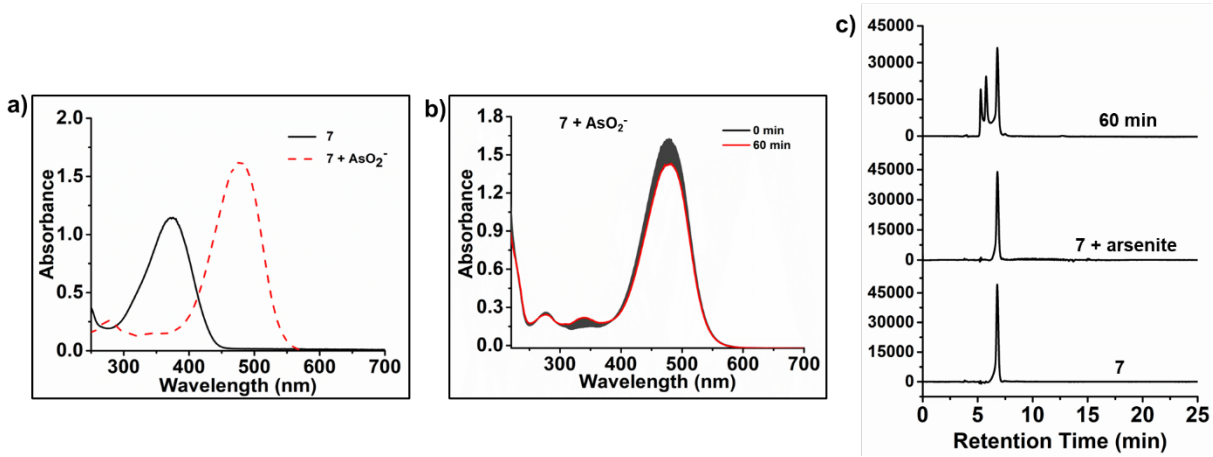

Figure S56. (a) Absorbance spectra of **7** with and without AsO_2^-; (b) time-dependent absorbance spectra of **7** with AsO_2^- (each trace was recorded after 1 min intervals); (c) HPLC chromatogram of **7** with AsO_2^-.

References

1. Shiraishi, Y.; Sumiya, S.; Kohno, Y.; Hirai, T. A Rhodamine-Cyclen Conjugate as a Highly Sensitive and Selective Fluorescent Chemosensor for Hg(II). *J. Org. Chem.* **2008**, *73*, 8571.